SCIENCE CHINA
Chemistry

•MINI REVIEWS•

February 2023 Vol.66 No.2: 315–323
https://doi.org/10.1007/s11426-021-1463-6

In situ/*operando* characterization techniques for electrochemical CO_2 reduction

Xinning Song[1,2,3], Liang Xu[1], Xiaofu Sun[1,3*] & Buxing Han[1,3,4*]

[1]*Beijing National Laboratory for Molecular Sciences, CAS Key Laboratory of Colloid and Interface and Thermodynamics, CAS Research/Education Center for Excellence in Molecular Sciences, Institute of Chemistry, Chinese Academy of Sciences, Beijing 100190, China;*
[2]*College of Science, China Agricultural University, Beijing 100193, China;*
[3]*School of Chemical Sciences, University of Chinese Academy of Sciences, Beijing 100049, China;*
[4]*Shanghai Key Laboratory of Green Chemistry and Chemical Processes, School of Chemistry and Molecular Engineering, East China Normal University, Shanghai 200062, China*

Received August 9, 2022; accepted November 18, 2022; published online January 9, 2023

Utilizing CO_2 as a carbon feedstock for producing fuels and useful chemicals is attractive due to the advantages of being abundant, nontoxic, and economical. Electrochemical CO_2 reduction (CO_2RR) provides an avenue to close the anthropogenic carbon cycle. However, the reaction process of multi-electronic products of CO_2RR is quite complex. It is hard to yield a target product with high selectivity, high current density, low overpotential, and good stability simultaneously. In recent years, *in situ*/*operando* characterization techniques have played important roles in the catalysis field *via* establishing the structure–reactivity/selectivity relationships of catalysts and thereby obtaining information about mechanisms. As a result, it is necessary to apply *in situ*/*operando* characterization technologies to clarify the reaction pathway of CO_2RR. In this mini-review, we discuss recent progress on the *in situ*/*operando* characterizations for electrochemical CO_2RR, including microscopies, infrared spectroscopy, Raman spectroscopy, X-ray photoelectron spectroscopy, and X-ray absorption fine spectroscopy. Moreover, the capabilities of these *in situ*/*operando* characterizations and the remaining challenges are also discussed.

carbon dioxide, electrocatalysis, *in situ*/*operando* characterization, catalyst design, reaction mechanism

Citation: Song X, Xu L, Sun X, Han B. *In situ*/*operando* characterization techniques for electrochemical CO_2 reduction. *Sci China Chem*, 2023, 66: 315–323, https://doi.org/10.1007/s11426-021-1463-6

1 Introduction

The energy utilization system based on traditional fossil fuels (coal, oil, natural gas, *etc*.) has caused an increasingly serious energy crisis and environmental problems, severely limiting the sustainable and healthy development of human society in the future [1,2]. The unrestrained combustion of fossil fuels also results in a continuous increase of CO_2 concentration in the atmosphere, which has led to numerous environment-related issues, such as global warming, ocean acidification, and the extinction of species [3–5]. Great efforts are being actively made to develop efficient approaches to reduce anthropogenic CO_2 emissions, which can be classified into CO_2 capture, storage, and utilization [6–8]. Using CO_2 as a carbon feedstock for producing fuels and useful chemicals is attractive due to the advantages of being abundant, nontoxic, and economical [9,10]. However, the high thermodynamic stability (with the high dissociation energy of C=O bonds, ~750 kJ mol^{-1}) and chemical inertness of CO_2 make it difficult to be activated. Different methods have been explored for CO_2 conversion, including chemical, electrochemical, photochemical, and biochemical transformations [11–15]. Electrochemical CO_2 reduction reaction (CO_2RR) is a promising approach by intermittently storing renewable solar

*Corresponding authors (email: sunxiaofu@iccas.ac.cn; hanbx@iccas.ac.cn)

© Science China Press 2023

and wind energy in carbon-based fuels and chemicals. Compared with other ways, electrochemical CO_2RR has mild reaction conditions, simple reaction units, controlled reaction process, and great potential for real industrial applications [16,17]. At present, a variety of target products (*e.g.*, CO, hydrocarbons, alcohols, and carboxylic acids) have been generated in heterogeneous/homogeneous catalysis process *via* a multiple-electron transfer [18–20]. It should be noted that hydrogen evolution reaction (HER) is usually competitive with CO_2RR, which greatly affects the Faradaic efficiency (FE) of CO_2RR [21,22]. Therefore, one of the key scientific problems is how to improve the selectivity of target products with the high current density, low overpotential and good stability simultaneously. However, the lack of clarity on the active sites and the unclear reaction pathway is the main hindrance towards the breakthrough of this field.

The mechanism of electrochemical CO_2RR is quite complex because it includes the transfer of multiple protons and electrons, as well as many different possible and complex reaction intermediates and products (Figure 1). Generally, the activation of CO_2 could be divided into the following four categories. * represents the surface-coordinated state of the catalyst.

$$*+H^++2e^-\rightarrow *H^- \quad (1)$$

$$*+CO_2+H^++e^-\rightarrow *OCOH \quad (2)$$

$$*+CO_2+H^++e^-\rightarrow *COOH \quad (3)$$

$$*+CO_2+e^-\rightarrow *CO_2^- \quad (4)$$

Formula (1) is the activation by means of an anionic hydrogen intermediate that exists in the process of formic acid production from CO_2RR catalyzed by molecular catalysts [23,24]. The anionic hydrogen acts as a nucleophilic reagent to attack CO_2 to produce formic acid. The catalytic process is usually achieved by modulating the oxidation state of the metal centers or ligands of the catalysts through the applied potential. Formulas (2) and (3) denote the proton-coupled electron transfer (PCET), which are commonly used to describe the transition and post-transition metals theoretically [25,26]. During CO_2RR, *OCHO is usually considered to be the most likely intermediate for HCOOH generation, while *COOH is the most likely intermediate for CO generation. Post-transition metals, such as Sn, Pb, and Bi, tend to bond with oxygen atoms in CO_2 to form formic acid, while transition metals, such as Zn, Ag, and Au, tend to bond with carbon atoms to form CO [27,28]. Formula (4) is the CO_2 activation mode regulated by electron transfer process, where $*CO_2^-$ bonds to the metal center. This mode is more sensitive to pH value than the mode of PCET, so pH can greatly affect the product selectivity in the catalytic system of this activation mode [29].

The reaction process of multi-electronic products of CO_2 RR is complex, so it is necessary to apply advanced technologies to study the reaction pathway of CO_2RR. On the other hand, more robust catalysts with the high efficiency

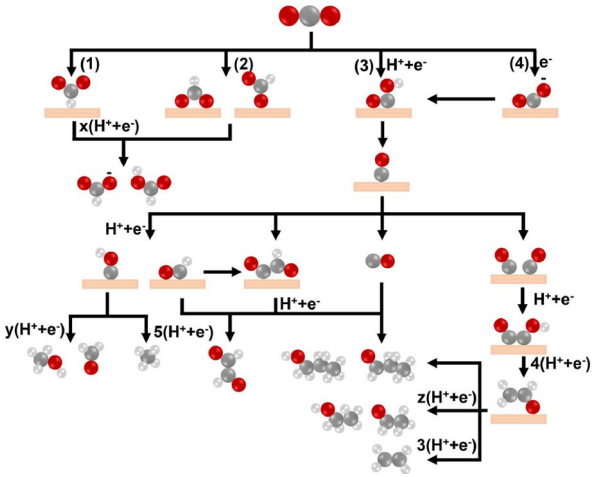


Figure 1 The possible pathways of different products during CO_2RR. The balls in grey, red and white represent C, O and H, respectively. x=0, formate; x=1, formic acid; y=1, formaldehyde; y=3, methanol; z=1, acetaldehyde; z=3, ethanol (color online).

and selectivity could be designed based on the mechanism of reactions. Up to date, some typical *ex situ* characterization technologies have been applied to explore the mechanism of CO_2RR, but very limited information can be obtained from these technologies [30,31]. Compared with the *ex situ* technologies, *in situ*/*operando* technologies have the advantages of real time, realism, and accuracy, and are more useful for determining the reaction mechanism and investigating structure–reactivity/selectivity relationships of catalysts [32,33]. Moreover, they are more conducive to capturing the intermediate state of the reaction. *In situ*/*operando* characterization techniques are used to reduce the *status quo* as much as possible under real reaction conditions to obtain accurate data to study the dynamic structure of catalysts on multiple time–space scales, and they are used to characterize catalysts as well as to analyze reaction products in real time [34]. In most cases, *in situ* and *operando* characterization techniques are used interchangeably. However, there is a slight difference: *in situ* (Latin, on site), where the reaction is monitored in real time at the positions relevant to the catalytic operation, not consistent with genuine reaction conditions, such as temperature, pressure; on the other hand, *operando* (Latin, working/operating), which indicates the operation under genuine reaction conditions, where the catalyst structure (active sites and intermediates), as well as activity and selectivity, is measured simultaneously in real time [35,36]. *In situ* techniques reveal the general properties of the catalysts, while *operando* techniques are particularly relevant for understanding the reaction mechanisms.

In this mini-review, we summarize recent progress on varieties of *in situ*/*operando* characterizations for electrochemical CO_2RR, mainly including microscopies, infrared (IR) spectroscopy, Raman spectroscopy, X-ray photoelectron spectroscopy (XPS) and X-ray absorption fine spectroscopy

(XAFS). The capabilities of these *in situ*/*operando* characterizations are also discussed. Additionally, the remaining challenges and some perspectives about using *in situ*/*operando* characterizations in CO_2RR are discussed.

2 Applications of *in situ*/*operando* techniques in electrochemical CO_2RR

Since the direct and definitive experimental proof of the mechanism of electrochemical CO_2RR is not available, the study of *in situ*/*operando* techniques and their application to the field of electrocatalysis is urgently needed [37, 38]. Compared with other electrocatalytic reactions, such as oxygen reduction reaction (ORR) and hydrogen evolution reaction (HER), CO_2RR involves the transfer of multiple electrons and the reaction process is more complicated, and the mechanism is not completely clear, so the applications of *in situ*/*operando* techniques for electrocatalytic reduction of CO_2 can better investigate the reaction mechanism. Therefore, the necessity of the using *in situ*/*operando* characterization technologies for CO_2RR includes: (1) in order to obtain specific products, it needs to study the catalysts' morphology, structure and intermediate. (2) *In situ*/*operando* technologies are used on the research of CO_2RR's further organic transformation, such as molecular activation and chemical bond reconstruction. (3) The results of *in situ*/*operando* technologies can be used to design the conditions of CO_2RR systems in the amplification and integration, including the influence of reaction conditions, reaction devices, electrochemical analysis methods.

The advantages and limitations of *in situ*/*operando* techniques are summarized in Table 1. Usually, the following experimental evidence can be provided *via in situ*/*operando* characterizations: (1) the observation of the morphology as well as the roughness of the catalyst; (2) the identification of key intermediates, such as *OCOH, *COOH; (3) observing the changes in the central atomic valence state of the catalyst and predicting the catalytic active site of the reaction; (4) predicting the reaction pathways and probing the bonding conditions, such as C–C coupling; (5) determining the stability and selectivity of catalysts in CO_2RR; (6) observing the environment-related effect on the reaction, such as the temperature, pressure, and solvent.

2.1 *In situ*/*operando* microscopies

In situ/*operando* microscopies are important techniques, mainly including scanning tunneling microscopy (STM), transmission electron microscopy (TEM), atomic force microscopy (AFM) [39–41]. They are used to observe directly at the atomic level the microstructural evolution and characterize the samples under the action of force, heat, electricity, magnetism during chemical reactions. The process of characterizations has been a popular field of materials-related research in recent years. For the *ex situ* electron microscopy, the experimental process is done outside the electron microscope, and then the sample is put into the electron microscope for the observation after the experiment is completed, and the changes that occurred in the sample during the experiment are inferred by comparing the images of the sample before and after the experiment. By contrast, the experimental process of the *in situ*/*operando* electron microscopy is completed in the electron microscope, and the

Table 1 The advantages and limitations of *in situ*/*operando* techniques

In situ/*operando* techniques	Advantages	Limitations
STM	Probing surface information of species	Requiring conductive or semiconductive surfaces
TEM	Tracking the changes in catalyst morphology	(1) Small imaging range (2) Operating conditions relatively strict (3) Sample preparation relatively strict
AFM	(1) Providing a true 3D surface view of the catalyst (2) No sample-processing required (3) Wide applicability (4) Obtaining surface morphology structure and surface roughness information with nanoscale resolution	(1) Small imaging range (2) Slow speed (3) Easy to be influenced by the probe
IR	(1) Determining changes in catalyst structure (2) Detecting reaction intermediates	Possible water peak interference
Raman	(1) Simple and highly accessible (2) Aqueous electrolytes can be used (3) Monitoring the catalyst state (4) Identifying intermediate species	(1) Limited spatial resolution (2) Less sensitive to changes in catalyst surface
XPS	(1) Probing electron transfer processes (2) Characterizing the element valence changes	(1) Conducted in ultra-high vacuum (2) Limited detection depth (1–10 nm)
XAFS	(1) Detecting catalyst valence changes (2) Detecting catalyst coordination environment	(1) Conducted in high-energy synchrotron (2) Describing average information of local structures (3) Difficulty in analyzing complex system components

experimental process is observed and recorded in real time as the experiment proceeds.

STM is an important tool for the extensive study of electrochemical processes at the nanoscale and allows the precise manipulation of atoms at low temperature (4 K) using a probe tip, which can observe and localize individual atoms [42,43]. Wan *et al*. [44] reported an *in situ*/*operando* STM study for CO_2RR catalyzed by cobalt phthalocyanine (CoPc). It is known that the ratio of CoPc–CO_2 complexes is correlated with the reduction of CoPc, and the contrast between CoPc–CO_2 and CoPc changes significantly. It also revealed that the formation of high contrast CoPc–CO_2 complexes at different potentials. This work provided the direct molecular evidence for understanding the mechanism of CO_2RR catalyzed by Co–N_4 sites. The relationship between the metal oxide interface and the enhanced activity of CO_2RR could be investigated by *in situ* STM [45]. The results showed that the Au–CeO_x interface played a dominant role in CO_2 adsorption and activation, which is further facilitated by the presence of –OH groups, and CO_2RR is greatly promoted by the adsorption of *COOH.

In situ/*operando* TEM can monitor the shape, size, and crystal structure of catalysts by imaging and diffraction techniques, which are important for understanding the catalytic structures under real reaction conditions and determining selectivity trends [46]. Wang *et al*. [41] found that, under applied bias conditions, CuO nanosheets slowly evolved into highly branched metallic Cu^0 dendrites (a dominant morphology under electrolyte flow conditions) by *in situ* TEM. The formation of cubic CuO particles from the copper sulfate solution during electrochemical synthesis and the morphological evolution of CuO at the reduction potential and electrode surface reconstruction can also be observed by *in situ* TEM [47]. In a word, the application of *in situ* TEM well tracks the morphological changes as well as the structural transformation of the catalyst under the real reaction conditions.

Electrochemical *in situ*/*operando* AFM is also a powerful tool for the real-time observation of changes in the catalyst surface morphology [39]. Kley *et al*. [48] used Cu (100) as the model surface, and measured the surface morphology during CO_2RR in 0.1 mol L^{-1} $KHCO_3$ *via in situ*/*operando* AFM (Figure 2). It was observed that the cathodic potential affected the surface significantly, which changed from granular to smooth curved mound pit surfaces or rectangular terraced structures. Advances in *in situ*/*operando* AFM further help the capture information on the dynamics of catalysts for CO_2RR.

2.2 *In situ*/*operando* IR spectroscopy

IR spectroscopy is used to measure the interaction of infrared radiation with the materials *via* absorption, emission, or reflection for studying and identifying chemical substances or functional groups [49]. *In situ*/*operando* IR technology is to record the micro-environment changes with an IR scanner [50]. The location and intensity of infrared absorption peaks help the determination of changes in the catalyst structure and the quantitative analysis of chemical group content during the reaction process to better simulate the experimental process and illustrate the reaction mechanism. Therefore, *in situ*/*operando* IR technology is widely used in CO_2RR.

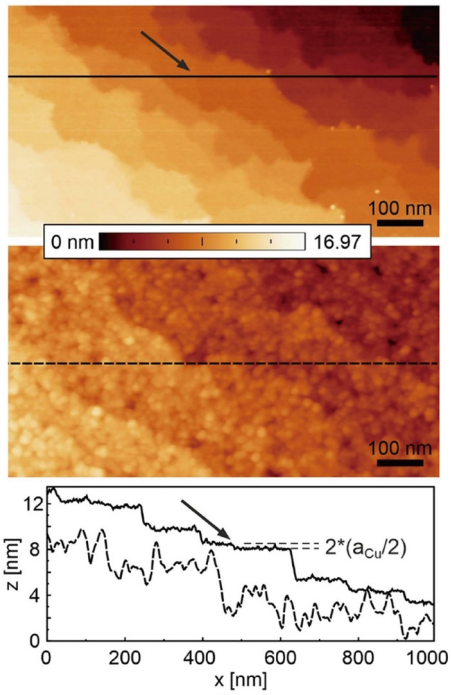


Figure 2 *Operando* AFM images for Cu (100) electrode surfaces during CO_2RR [48] (color online).

In situ IR spectroscopy can be used for monitoring the dynamic evolution of the adsorbed intermediate, *CO. Wei *et al*. [51] used *in situ* IR spectroscopy to find that the antisymmetric stretching vibrational peaks of O–H bonds in H_2O molecules on the surface of Cu–PANI electrode were significantly lower than those on the surface of Cu electrodes, which indicated that the polyaniline on the surface of Cu–PANI electrodes inhibited the adsorption of H_2O molecules and reduced the HER and in turn improved the FE of multicarbon products. Meanwhile, the absorption peaks of intermediate *CO-related absorption peaks were stronger on the surface of Cu–PANI electrodes, indicating that the higher surface coverage of *CO promoted the formation of polycarbonate products by *CO–*CO coupling. In addition, Gong *et al*. [52] used attenuated-total-reflection surface-enhanced infrared absorption spectroscopy (ATR–SEIRAS) to investigate the effect of Cu crystalline facets on the intermediate adsorption. The results demonstrated that the Cu (100) surface might be a strong *CO adsorption site, thus

maintaining a higher CO surface coverage and giving the catalyst a higher C–C coupling performance.

In addition, *in situ* FTIR spectroscopy is an important tool for identifying intermediates and revealing reaction pathways. Koper's group [53] has detected a hydrogenated CO dimer intermediate by *in situ* FTIR. The results showed that Cu (100) electrodes host a C-containing absorbate with vibrational bands (1,191/1,584 cm^{-1}) at low overpotentials (Figure 3). Combined with the density functional theory (DFT) calculations, the bands were considered to be the C–O–H and carbonyl bond stretching modes of the CO dimer intermediate (OCCOH). This study is the first time to achieve the direct verification of OCCOH intermediate hypothesis of CO_2RR on Cu. Furthermore, Ma *et al*. [54] investigated the changes of reaction intermediates on F–Cu catalysts using *in situ* FTIR spectroscopy. As potential became more negative, a new peak was detected on the F–Cu catalyst (1,754 cm^{-1}), which corresponds to the crucial intermediate *CHO in the CO_2RR process, thus providing strong experimental evidence for the proposed mechanism of the *CHO–*CHO coupling.

Interestingly, *in situ* FTIR spectroscopy can also determine the magnitude of the electrode surface pH. Using *in situ* FTIR spectroscopy, Zhu *et al*. [55] could directly monitor the reaction intermediates (*CO, *CHO, *COOH, bidentate COO^-) and determine the magnitude of the electrode surface pH based on the ratio of HCO_3^- and CO_3^{2-} adsorbed on the electrode surface.

In conclusion, *in situ* FTIR can monitor the adsorption and desorption behavior of intermediates on the electrode surface, the evolution of the electrode structure and the electrode surface microenvironment in real time at the molecular level, which is important for catalyst design, reaction mechanism investigation, and electrode surface microenvironment regulation.

2.3 *In situ*/*operando* Raman spectroscopy

Similar to IR spectroscopy, Raman spectroscopy is a spectroscopic technique typically used to determine vibrational modes of molecules, although the rotational and other low-frequency modes of systems may also be observed. Since the *in situ*/*operando* techniques usually involve the immersion of the electrode surface in a liquid electrolyte in operation, Raman spectroscopy is feasible due to the low Raman scattering of water. To some extent, Raman spectroscopy and IR are complementary. The catalysts with symmetric molecular centers can be detected using *operando* Raman techniques, while molecules with asymmetric centers are more appropriately detected using *operando* IR techniques.

Operando Raman spectroscopy often applied the surface-enhanced Raman scattering (SERS) effect, especially focusing on the top of certain roughened metals' weak scattering cross-sections [56,57]. Raman spectroscopy's feature of high-speed data acquisition makes it suitable to identify and monitor the intermediates and the metastable catalyst states. Thus, in recent years, there have been two kinds of applications of *operando* SERS in CO_2RR: (1) monitoring the catalyst state; (2) intermediate species identification.

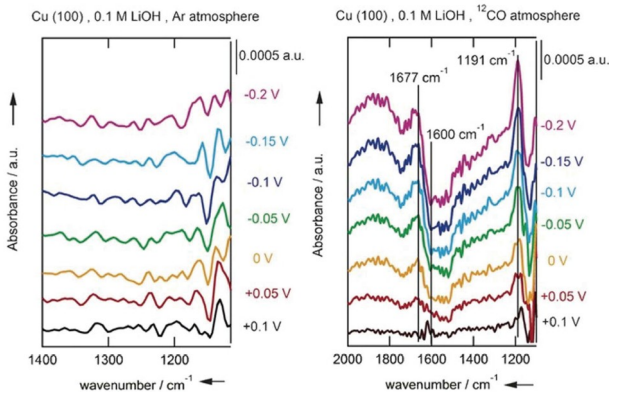


Figure 3 *Operando* IR spectra for Cu (100) at different potentials during CO_2RR [53] (color online).

Operando Raman spectroscopy contributes to monitoring the catalyst structure transition. Zhou *et al*. [58] applied the *operando* Raman technique to detect the change of catalyst valence states. The transformation of Ce^{4+} to Ce^{3+} in Cu–Ce–O_x was confirmed by the appearance of a new peak at ~560 cm^{-1} during the negative scan. The peak originated from the oxygen vacancy formed by the valence state changes of Ce. It was found that the conversion of Ce^{4+} to Ce^{3+} during the reaction and Ce^{3+} could stabilize the Cu^{2+} active site. In addition, the stability of the catalyst structure can be probed using *in situ* Raman spectroscopy. The Raman peaks (assigned to the Sn–O bond) appeared at 630 cm^{-1} for both SnO_2 and F-SnO_2 at applied potentials from −0.4 to −0.8 V [59]. As the applied potential increased, the Sn–O on F-SnO_2 remained stable, while the Sn–O peak on SnO_2 was almost negligible, indicating that the doping of the F element was beneficial to maintain the stability of the SnO_2 structure. Broekmann *et al*. [60] monitored the gradual transition of the carbonate/oxide composite catalyst to its all-metallic state using *operando* Raman spectroscopy. For the first time, experimental evidence was provided for the embedding of CO_2 into oxidized Bi_2O_3 substrates at low overpotential during the reaction.

Another important role of *operando* Raman spectroscopy is to identify intermediate species. Based on a comprehensive suite of experimental and theoretical study, Chernyshova's group [61] has established a theory of the formation of a carboxylate intermediate on Cu in the CO_2RR process. From the *operando* Raman spectra (Figure 4a), some main peaks can be assigned to *CO, *CO_3^{2-} and *CO_2^-. Gratzel's group [62] has also used *operando* Raman spectroscopy to gain mechanistic insight into the catalytic differences be-

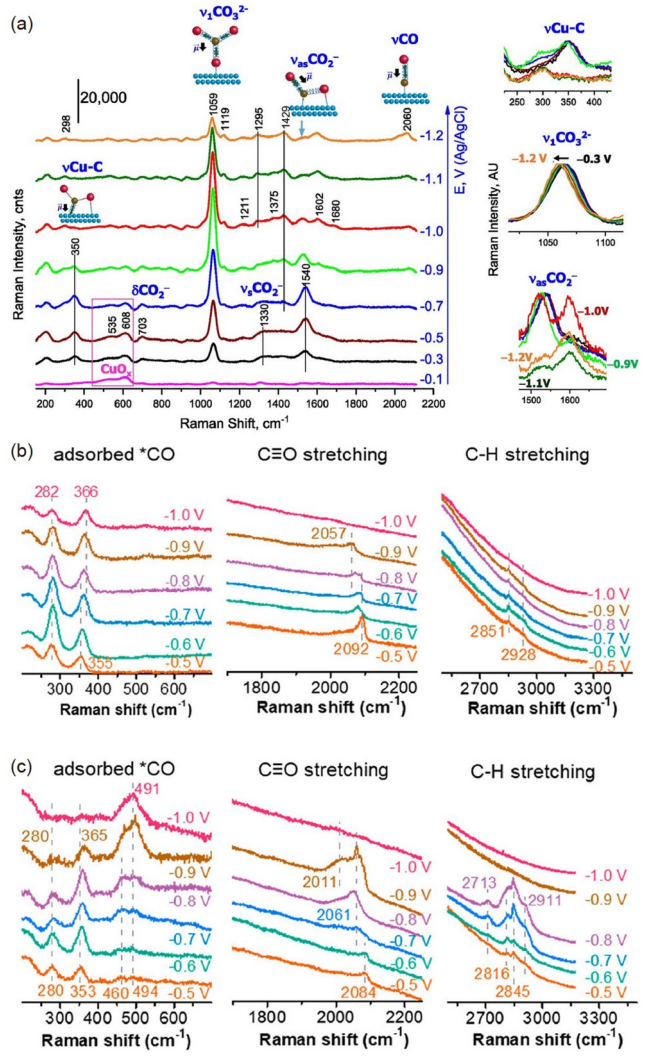


Figure 4 (a) *Operando* SERS of rough Cu surface in CO_2-saturated in 0.1 mol L^{-1} $NaHCO_3$ (pH 6.8) [61]. *Operando* Raman spectra of (b) Cu and (c) CuAg during CO_2RR at different potentials [62] (color online).

tween Cu and CuAg during CO_2RR (Figure 4b and 4c). The peaks located at ~2,850 and ~2,920 cm^{-1} on the CuAg catalyst are more pronounced than that on Cu, and new peaks appear at 2,713 and 2,816 cm^{-1}, suggesting that more C–H-bonded intermediates (such as *CHO, $*C_2H_2O$) are present on the surface. It well explained the enhanced activity of ethylene and other C_{2+} products on CuAg. In addition, *operando* Raman spectroscopy could be used to quantify the coverage of surface intermediates during the reaction. Cuenya's group [63] used it to track the surface coverage of Cu_2O reaction intermediates and found that the ratio of Cu–CO stretching band to CO rotational band varied with the applied potential and was closely related to the CO coverage, thus affecting the degree of C–C coupling.

The *operando* Raman spectroscopy studies provide important information on the identification of intermediate species and the nature of catalytic active sites, which is essential for the investigation of reaction mechanisms. However, the low spatial resolution (nanoscale) and sensitivity (low signal-to-noise ratio) to the catalyst surface evolution limit it to provide more information. Therefore, it is necessary to use *in situ* XAS, XPS and other techniques for mutual validation and complementation.

2.4 *In situ*/*operando* XPS spectroscopy

XPS is based on the photoelectric effect as a surface-sensitive quantitative spectroscopic technique, and it can identify material surface elements, chemical state, and electronic structure, *etc*. However, *operando* XPS characterization is restricted due to the requirement of an ultra-high vacuum. Thus, only *quasi-operando* studies have been conducted through an adjacent XPS chamber without exposing the sample to air.

Quasi-operando XPS can probe the transformation of electronic structures and the changes in the valence state of elements. Our group revealed the nature of the electron density reconfiguration of atomically dispersed In catalysts by *quasi-operando* XPS [64]. From the *quasi-operando* XPS analysis of O 1s, it was clear that the area of the two peaks at 533.4 eV (corresponding to physically adsorbed CO_2) and 532.3 eV (corresponding to chemically adsorbed CO_2^-) increased after the reaction. This provided the direct evidence for the charge transport on In_A/NC and the formation of the key intermediate, CO_2^-. As seen in Figure 5 [64], the In 3d peak of In_A/NC moved toward a higher binding energy compared with those of other catalysts, which indicated that its surface species had a higher oxidation state. At the same time, the In MNN Auger line position of In_A/NC was observed at approximately 406.8 eV, indicating that In was in the form of oxides. Besides, we also used *quasi-operando* XPS to monitor Cu-based catalysts during CO_2RR [65]. Furthermore, *in situ* XPS technique was used to detect the valence change of Cu-based catalysts under electroreduction, which provided the evidence for the strong relationship between catalyst structure and product selectivity [66].

2.5 *In situ*/*operando* XAFS

XAFS is mainly used to measure local electronic structures, and it is divided into two main categories: X-ray absorption near-edge structure (XANES) and extended X-ray absorption fine structure (EXAFS). The former is often used to provide the information on the chemical state and geometry of the adsorbed atoms, while the latter is used to get the information on the near-neighbor coordination structure of the adsorbed atoms.

In situ XAFS can detect valence changes of catalyst elements, monitor catalyst reconfiguration during the electrolysis, and determine the active site of catalysts to better

explain the structure–reactivity relationship. For example, the transient transition from single-site Cu to metallic Cu nanoparticles can be observed *via operando* XAFS [67]. Figure 6 showed a shift in the edge position, indicating the change of Cu oxidation state from +2 to 0 under electrocatalytic conditions. When moderate potentials (from −0.6 V *vs*. RHE) were applied, Cu–Cu coordination immediately appeared, suggesting that metallic Cu nanoparticles extensively formed. Cu nanoparticles converted from Cu–N_4 in the electrolysis may be the active site of catalysts, exhibiting the unique reactivity (producing only one kind of liquid products, ethanol). Similarly, Wang *et al*. [68] reported that atomically dispersed Cu atoms were converted to Cu_n clusters during CO_2RR in a reversible way as observed by *operando* XAS. The FE of ethanol was high when Cu was present in the form of atomic dispersion, while it decreased significantly when CuO and Cu clusters were dominated. The study on catalyst valence and catalyst reconfiguration during CO_2RR provides the guidance for the identification of the true catalytic active site and the study of structure–activity/selectivity relationships.

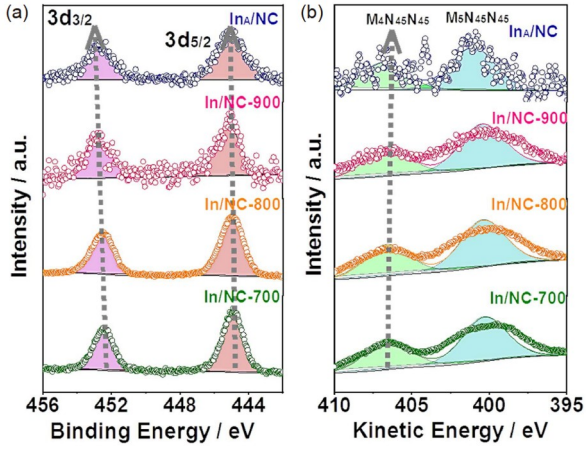


Figure 5 *Quasi-operando* XPS spectra of (a) In 3d orbits and (b) In MNN Auger spectra of different catalysts [64] (color online).

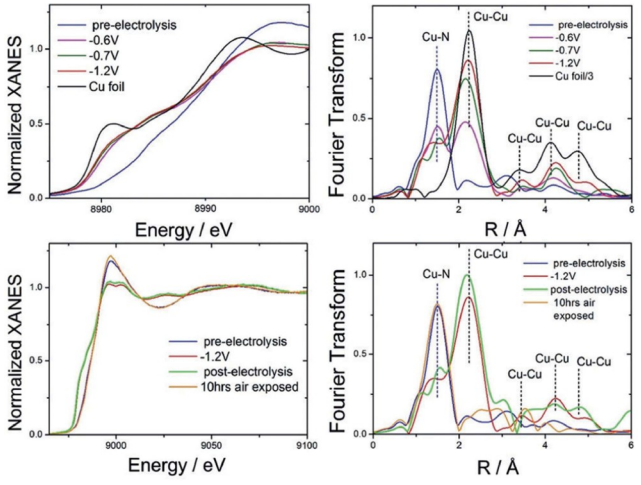


Figure 6 *Operando* XAS characterizations of Cu-based catalysts during CO_2RR [67] (color online).

By studying the local coordination environment using *in situ* XAS, it is easy to gain a deeper understanding of the structure–activity relationship at the atomic level. The structural evolution of the Ni–N_4 site in atomically dispersed N-doped graphene (A–Ni–NG) was also studied by *in situ* XAFS [69]. The EXAFS spectrum of A–Ni–NG shows a shift of the main peak at 1.45 Å (assigned to the Ni–N bond) to a longer length of 0.04 Å during the electrolysis, indicating an extension of the Ni–N bond. The change in the Ni–N bond length was due to the deformation of Ni atoms outside the graphene plane caused by the electron redistribution in the Ni 3d orbitals. *In situ* XAS was also used to determine the structural evolution of Fe–N sites [70]. From −0.4 to −0.5 V *vs*. RHE, the FE of CO_2 to CO conversion decreased. Meanwhile, the Fe K edge XANES of Fe^{3+}–N–C-based single-atomic catalysts shifted lower and the coordination number for Fe–pyrrolic N changed from 4 to 3. It indicated the reduction of Fe^{3+} to Fe^{2+} in CO_2RR, thus proving that Fe^{3+} rather than Fe^{2+} is the active center of catalysis. The *in situ* XAFS allows to know the change of the bond length and coordination number of catalysts during the reaction and thus the reason for the change of catalytic activities.

3 Summary and outlook

In summary, some *in situ*/*operando* techniques have been successfully used for studying CO_2RR, such as microscopy (TEM and AFM), optical spectroscopy (IR and Raman), and some X-ray based characterizations (XPS and XAFS). Through these *in situ*/*operando* technologies, we have gained a deeper understanding of the electrocatalytic process, such as monitoring the structure, morphology and chemical states of catalysts, reaction intermediates, products. Furthermore, the *in situ*/*operando* characterization provides the guidance for the subsequent design of the catalyst and plays a crucial role for the future large-scale and efficient utilization of the catalyst on CO_2RR.

Despite the impressive progress achieved, there are still multiple issues that hinder the full understanding of electrocatalytic CO_2RR.

(1) Improving the detection capability of *in situ*/*operando* technologies. The existing *operando* techniques have certain problems, such as the detection signals of *operando* IR and Raman may be more disturbed by water-related peaks or other impurity-related peaks. Therefore, for the further advancement, signal intensities of the characterization techniques are needed to be improved.

(2) Developing new *in situ*/*operando* technologies. The

gap between operational cells designed and real devices still remains, and it needs to be close through the particular technologies. Some *in situ*/*operando* techniques are difficult to reach the real environment, such as *quasi-operando* XPS, while some suitable techniques require harsh experimental conditions, such as *in situ*/*operando* TEM which requires an ultra-vacuum [33]. Therefore, the development of new *in situ* techniques for the active site identification and the inference of reaction mechanisms can be considered.

(3) Combining various *in situ*/*operando* techniques. The combination of various *in situ*/*operando* characterization techniques is expected to study the structure, electronic state of the catalysts, and reaction intermediates in the same reaction process, so that we can get insight into the structure–activity relationship of the catalysts and the reaction mechanism [30]. *In situ*/*operando* technology has also driven technological advances because of the need for relevant technologies. In the future, a number of combined *operando* techniques will allow a better understanding of the reaction process.

(4) Combining theoretical calculations and *in situ* techniques for the mechanism analysis. In addition to predicting the adsorption energy of key reaction intermediates, *in situ* theoretical calculations critically need to consider the real electrochemical environment of the catalysts such as local pH, electrode potential. *In situ* theoretical calculations play an important role in understanding the reaction mechanism. By combining *operando* calculations and *operando* spectroscopy, as well as electrochemical tests, the specific mechanisms of C_2 and C_{2+} product formation can be more comprehensively explored, especially the C–C coupling process [30]. In addition, machine learning can simulate the whole reaction process and predict the dynamic evolution of CO_2RR. Combining machine learning with *operando* techniques is expected to greatly improve research efficiency.

Acknowledgements This work was supported by National Natural Science Foundation of China (22002172, 22121002), Beijing Natural Science Foundation (J210020), National Key Research and Development Program of China (2020YFA0710203), Chinese Academy of Sciences (QYZDY-SSW-SLH013) and Photon Science Center for Carbon Neutrality.

Conflict of interest The authors declare no conflict of interest.

1 Shindell D, Smith CJ. *Nature*, 2019, 573: 408–411
2 Lu L, Sun X, Ma J, Zhu Q, Wu C, Yang D, Han B. *Sci China Chem*, 2018, 61: 228–235
3 Jiang X, Nie X, Guo X, Song C, Chen JG. *Chem Rev*, 2020, 120: 7984–8034
4 Yang D, Zhu Q, Han B. *Innovation*, 2020, 1: 100016
5 Xu L, Ma X, Wu L, Tan X, Song X, Zhu Q, Chen C, Qian Q, Liu Z, Sun X, Liu S, Han B. *Angew Chem Int Ed*, 2022, 61: e202210375
6 He M, Sun Y, Han B. *Angew Chem Int Ed*, 2022, 61: e202112835
7 Tan X, Guo W, Liu S, Jia S, Xu L, Feng J, Yan X, Chen C, Zhu Q, Sun X, Han B. *Chem Sci*, 2022, 13: 11918–11925
8 Zhang L, Dang Y, Zhou X, Gao P, Petrus van Bavel A, Wang H, Li S, Shi L, Yang Y, Vovk EI, Gao Y, Sun Y. *Innovation*, 2021, 2: 100170
9 Song X, Guo W, Ma X, Xu L, Tan X, Wu L, Jia S, Wu T, Ma J, Zhang F, Jia J, Sun X, Han B. *Green Chem*, 2022, 24: 1488–1493
10 Ma X, Xu L, Liu S, Zhang L, Tan X, Wu L, Feng J, Liu Z, Sun X, Han B. *Chem Catal*, 2022, 2: 3207–3224
11 Huang JE, Li F, Ozden A, Sedighian Rasouli A, García de Arquer FP, Liu S, Zhang S, Luo M, Wang X, Lum Y, Xu Y, Bertens K, Miao RK, Dinh CT, Sinton D, Sargent EH. *Science*, 2021, 372: 1074–1078
12 Jiao X, Zheng K, Chen Q, Li X, Li Y, Shao W, Xu J, Zhu J, Pan Y, Sun Y, Xie Y. *Angew Chem Int Ed*, 2020, 59: 15497–15501
13 Ren X, Liu S, Li H, Ding J, Liu L, Kuang Z, Li L, Yang H, Bai F, Huang Y, Zhang T, Liu B. *Sci China Chem*, 2020, 63: 1727–1733
14 Gao D, Wei P, Li H, Lin L, Wang G, Bao X. *Acta Physico Chim Sin*, 2021, 37: 2009021
15 Wang H, Wu Y, Zhao Y, Liu Z. *Acta Physico Chim Sin*, 2021, 37: 2010022
16 Zhong D, Zhao ZJ, Zhao Q, Cheng D, Liu B, Zhang G, Deng W, Dong H, Zhang L, Li J, Li J, Gong J. *Angew Chem Int Ed*, 2021, 60: 4879–4885
17 Tan X, Sun X, Han B. *Natl Sci Rev*, 2022, 9: nwab022
18 Jin S, Hao Z, Zhang K, Yan Z, Chen J. *Angew Chem Int Ed*, 2021, 60: 20627–20648
19 Xiong L, Zhang X, Chen L, Deng Z, Han S, Chen Y, Zhong J, Sun H, Lian Y, Yang B, Yuan X, Yu H, Liu Y, Yang X, Guo J, Rümmeli MH, Jiao Y, Peng Y. *Adv Mater*, 2021, 33: 2101741
20 Zhao Y, Zu X, Chen R, Li X, Jiang Y, Wang Z, Wang S, Wu Y, Sun Y, Xie Y. *J Am Chem Soc*, 2022, 144: 10446–10454
21 Li P, Bi J, Liu J, Zhu Q, Chen C, Sun X, Zhang J, Han B. *Nat Commun*, 2022, 13: 1965
22 Wu Y, Chen C, Yan X, Sun X, Zhu Q, Li P, Li Y, Liu S, Ma J, Huang Y, Han B. *Angew Chem Int Ed*, 2021, 60: 20803–20810
23 Wu Y, Cao S, Hou J, Li Z, Zhang B, Zhai P, Zhang Y, Sun L. *Adv Energy Mater*, 2020, 10: 2000588
24 Zhang E, Wang T, Yu K, Liu J, Chen W, Li A, Rong H, Lin R, Ji S, Zheng X, Wang Y, Zheng L, Chen C, Wang D, Zhang J, Li Y. *J Am Chem Soc*, 2019, 141: 16569–16573
25 Liang S, Huang L, Gao Y, Wang Q, Liu B. *Adv Sci*, 2021, 8: 2102886
26 Li M, Garg S, Chang X, Ge L, Li L, Konarova M, Rufford TE, Rudolph V, Wang G. *Small Methods*, 2020, 4: 2000033
27 Xie W, Li H, Cui G, Li J, Song Y, Li S, Zhang X, Lee JY, Shao M, Wei M. *Angew Chem Int Ed*, 2021, 60: 7382–7388
28 Yi L, Chen J, Shao P, Huang J, Peng X, Li J, Wang G, Zhang C, Wen Z. *Angew Chem Int Ed*, 2020, 59: 20112–20119
29 Peng H, Tang MT, Liu X, Lamoureux PS, Bajdich M, Abild-Pedersen F. *Energy Environ Sci*, 2021, 14: 473–482
30 Li X, Wang S, Li L, Sun Y, Xie Y. *J Am Chem Soc*, 2020, 142: 9657–9581
31 Jiao X, Hu Z, Li L, Wu Y, Zheng K, Sun Y, Xie Y. *Sci China Chem*, 2022, 65: 428–440
32 Zou Y, Wang S. *Adv Sci*, 2021, 8: 2003579
33 Cao X, Tan D, Wulan B, Hui KS, Hui KN, Zhang J. *Small Methods*, 2021, 5: 2100700
34 Vavra J, Shen TH, Stoian D, Tileli V, Buonsanti R. *Angew Chem Int Ed*, 2021, 60: 1347–1354
35 Bañares MA. *Catal Today*, 2005, 100: 71–77
36 Yang Y, Xiong Y, Zeng R, Lu X, Krumov M, Huang X, Xu W, Wang H, DiSalvo FJ, Brock JD, Muller DA, Abruña HD. *ACS Catal*, 2021, 11: 1136–1178
37 Handoko AD, Wei F, Jenndy F, Yeo BS, Seh ZW. *Nat Catal*, 2018, 1: 922–934
38 Li J, Gong J. *Energy Environ Sci*, 2020, 13: 3748–3779
39 Grosse P, Gao D, Scholten F, Sinev I, Mistry H, Roldan Cuenya B. *Angew Chem Int Ed*, 2018, 57: 6192–6197
40 Phan TH, Banjac K, Cometto FP, Dattila F, García-Muelas R, Raaijman SJ, Ye C, Koper MTM, López N, Lingenfelder M. *Nano Lett*, 2021, 21: 2059–2065
41 Wang X, Klingan K, Klingenhof M, Möller T, Ferreira de Araújo J,

Martens I, Bagger A, Jiang S, Rossmeisl J, Dau H, Strasser P. *Nat Commun*, 2021, 12: 794
42 Jacobse L, Huang YF, Koper MTM, Rost MJ. *Nat Mater*, 2018, 17: 277–282
43 Pfisterer JHK, Liang Y, Schneider O, Bandarenka AS. *Nature*, 2017, 549: 74–77
44 Wang X, Cai ZF, Wang YQ, Feng YC, Yan HJ, Wang D, Wan LJ. *Angew Chem Int Ed*, 2020, 59: 16098–16103
45 Gao D, Zhang Y, Zhou Z, Cai F, Zhao X, Huang W, Li Y, Zhu J, Liu P, Yang F, Wang G, Bao X. *J Am Chem Soc*, 2017, 139: 5652–5655
46 Beermann V, Holtz ME, Padgett E, de Araujo JF, Muller DA, Strasser P. *Energy Environ Sci*, 2019, 12: 2476–2485
47 Arán-Ais RM, Rizo R, Grosse P, Algara-Siller G, Dembélé K, Plodinec M, Lunkenbein T, Chee SW, Cuenya BR. *Nat Commun*, 2020, 11: 3489
48 Simon GH, Kley CS, Roldan Cuenya B. *Angew Chem Int Ed*, 2021, 60: 2561–2568
49 Dang S, Qin B, Yang Y, Wang H, Cai J, Han Y, Li S, Gao P, Sun Y. *Sci Adv*, 2020, 6: eaaz2060
50 Zhang CC, Shi J, Hartlaub S, Palamara JP, Petrovic I, Yilmaz B. *Catal Commun*, 2021, 150: 106273
51 Wei X, Yin Z, Lyu K, Li Z, Gong J, Wang G, Xiao L, Lu J, Zhuang L. *ACS Catal*, 2020, 10: 4103–4111
52 Zhang G, Zhao ZJ, Cheng D, Li H, Yu J, Wang Q, Gao H, Guo J, Wang H, Ozin GA, Wang T, Gong J. *Nat Commun*, 2021, 12: 5745
53 Pérez-Gallent E, Figueiredo MC, Calle-Vallejo F, Koper MTM. *Angew Chem Int Ed*, 2017, 56: 3621–3624
54 Ma W, Xie S, Liu T, Fan Q, Ye J, Sun F, Jiang Z, Zhang Q, Cheng J, Wang Y. *Nat Catal*, 2020, 3: 478–487
55 Zhu S, Jiang B, Cai WB, Shao M. *J Am Chem Soc*, 2017, 139: 15664–15667
56 Chen S, Li WH, Jiang W, Yang J, Zhu J, Wang L, Ou H, Zhuang Z, Chen M, Sun X, Wang D, Li Y. *Angew Chem Int Ed*, 2022, 61: e202114450
57 Wang J, Tan HY, Zhu Y, Chu H, Chen HM. *Angew Chem Int Ed*, 2021, 60: 17254–17267
58 Zhou X, Shan J, Chen L, Xia BY, Ling T, Duan J, Jiao Y, Zheng Y, Qiao SZ. *J Am Chem Soc*, 2022, 144: 2079–2084
59 Ko YJ, Kim JY, Lee WH, Kim MG, Seong TY, Park J, Jeong YJ, Min BK, Lee WS, Lee DK, Oh HS. *Nat Commun*, 2022, 13: 2205
60 Dutta A, Montiel IZ, Kiran K, Rieder A, Grozovski V, Gut L, Broekmann P. *ACS Catal*, 2021, 11: 4988–5003
61 Chernyshova IV, Somasundaran P, Ponnurangam S. *Proc Natl Acad Sci USA*, 2018, 115: E9261–E9270
62 Gao J, Zhang H, Guo X, Luo J, Zakeeruddin SM, Ren D, Grätzel M. *J Am Chem Soc*, 2019, 141: 18704–18714
63 Zhan C, Dattila F, Rettenmaier C, Bergmann A, Kühl S, García-Muelas R, López N, Cuenya BR. *ACS Catal*, 2021, 11: 7694–7701
64 Guo W, Tan X, Bi J, Xu L, Yang D, Chen C, Zhu Q, Ma J, Tayal A, Ma J, Huang Y, Sun X, Liu S, Han B. *J Am Chem Soc*, 2021, 143: 6877–6885
65 Chen C, Sun X, Yan X, Wu Y, Liu M, Liu S, Zhao Z, Han B. *Green Chem*, 2020, 22: 1572–1576
66 Su X, Jiang Z, Zhou J, Liu H, Zhou D, Shang H, Ni X, Peng Z, Yang F, Chen W, Qi Z, Wang D, Wang Y. *Nat Commun*, 2022, 13: 1322
67 Karapinar D, Huan NT, Ranjbar Sahraie N, Li J, Wakerley D, Touati N, Zanna S, Taverna D, Galvão Tizei LH, Zitolo A, Jaouen F, Mougel V, Fontecave M. *Angew Chem Int Ed*, 2019, 58: 15098–15103
68 Weng Z, Wu Y, Wang M, Jiang J, Yang K, Huo S, Wang XF, Ma Q, Brudvig GW, Batista VS, Liang Y, Feng Z, Wang H. *Nat Commun*, 2018, 9: 415
69 Yang HB, Hung SF, Liu S, Yuan K, Miao S, Zhang L, Huang X, Wang HY, Cai W, Chen R, Gao J, Yang X, Chen W, Huang Y, Chen HM, Li CM, Zhang T, Liu B. *Nat Energy*, 2018, 3: 140–147
70 Gu J, Hsu CS, Bai L, Chen HM, Hu X. *Science*, 2019, 364: 1091–1094
71 Zheng Y, Vasileff A, Zhou X, Jiao Y, Jaroniec M, Qiao SZ. *J Am Chem Soc*, 2019, 141: 7646–7659